RESEARCH PAPER
PCCP
www.rsc.org/pccp

Time-resolved total internal reflection fluorescence spectroscopy

Part I. Photophysics of Coumarin 343 at liquid/liquid interface

Debi Pant and Hubert H. Girault

Laboratoire d'Electrochimie, Ecole Polytechnique Fédérale de Lausanne, CH-1015 Lausanne, Switzerland

Received 6th June 2005, Accepted 29th July 2005
First published as an Advance Article on the web 22nd August 2005

Pico-second time-resolved time-correlated single photon counting (TCSPC) technique under the total internal reflection (TIR) condition has been used to study the photophysical properties of Coumarin 343 (C343) dye molecules adsorbed at the water/1,2-dichloroethane (DCE) interface. The fluorescence decay profile of C343 under TIR condition at the water/DCE interface was non-exponential and fitted to the double exponential decay function with the fluorescence lifetimes 0.3 and 3.6 ns, which proved the existence of two different forms of C343 species having largely different lifetimes at the interface. The longer fluorescence lifetime component of C343 at the interface is attributed to the emission from the monomeric form of the dye molecules and the shorter lifetime component is due to the aggregation of dye molecules. The penetration depth dependence of decay curves indicated no change in the fluorescence lifetime components, however, the amplitude corresponding to the lifetime of aggregate increased and the amplitude corresponding to the lifetime of monomer decreased with the decrease in penetration depth of the aqueous phase from the interface. Aggregation is significant in the interfacial layer. The decrease in monomer lifetime at the interface compared to that in the bulk solution is interpreted in terms of excitation energy migration between the dye molecules.

1. Introduction

Total internal reflection (TIR) is a well established and powerful optical technique to obtain information about the interaction of molecules with surfaces and interfaces. When a beam of light is incident at an angle greater than the critical angle onto an interface between two transparent media having different indices of refraction, the beam totally internally reflects at the interface between the two media. At the point of TIR, an evanescent wave penetrates into the medium. The evanescent wave which penetrates from a higher into a lower refractive index material under TIR has been used[1–16] to excite fluorophores selectively at the surfaces and interfaces with relatively little penetration into the bulk.

TIR fluorescence spectroscopy has been used to understand the structure and dynamics of solid/liquid interfaces.[1–4,7,8,13–19] Hamai *et al.*[1] studied the inhomogeneous aggregation of a Merocyanine dye at the solid/liquid interface layer as a function of penetration depth of the evanescent wave intensity. They also studied[2] the excited-state proton transfer reaction of 1-naphthol at the sapphire/water interface. The rate constant of the excited-state proton transfer reaction of 1-naphthol at the interface layer was reduced as compared to that in a bulk aqueous solution. In another study Hamai *et al.*[17] investigated the effects of the solid/liquid interface on the excimer formation of pyrene in toluene containing poly(methyl methacrylate) and the rise and decay rates of the excimer fluorescence were decelerated in a sapphire/toluene interface layer. These findings were interpreted by an increase in the viscosity of the interface layer. Masuhara and coworkers[7] used TIR sub-nanosecond fluorescence spectroscopy for elucidating photophysical and photochemical processes of a polymer surface. The thickness which could be studied under the experimental conditions used was of the order of 0.01 μm. In another study Masuhara and coworkers[8] used a sapphire plate as an internal reflection element, and a model system composed of thin and thick polystyrene films was prepared. Both films contained different dopants whose fluorescence spectra rise, as well as decay, curves were investigated as a function of an incident angle. A difference between theory prediction and experimental results was ascribed to beam divergence, flatness of optics, and optical condition of the films. Fluorescence rise and decay components of Coumarin 460 in the 1-BuOH/sapphire interface layer were slower in the interface layer compared to that in the bulk and the results have been interpreted in terms of the longitudinal relaxation of 1-BuOH affected by H-bonding interactions between the hydrophilic sapphire surface and 1-BuOH.[16] Kitamura and coworkers[15] have studied photoisomerization of 3,3′-diethyloxadicarbocyanine iodide (DODCI) between the N and P isomers at bare borosilicate and octadecyl chain-modified C18 glass/ethanol interfaces. Both the fluorescence spectrum and the lifetime of DODCI detected at the glass/ethanol interface were different from those in bulk ethanol. The large decrease in the isomerization rate was explained in terms of an increase in local friction (viscosity) at the interface and strong structural interactions between DODCI and the octadecyl chains bound to the glass surface.

While much less is known about the structural and dynamical properties of the surfaces and interfaces, a few studies have been reported in order to understand the structure and dynamics of the liquid/liquid interfaces. Bessho *et al.*[20] have used pico-second time-resolved TIR fluorescence spectroscopy to study the microenvironments of 8-anilino-1-naphthalenesulfonate molecules at the heptane/water interface. Their measurements of fluorescence decay indicated that the fluorophores in the vicinity of the interface were present in two different solvated structures. One of them was located up to a few nanometers from the interface, and the other was located in a relatively wide range towards the aqueous phase. Fujiwara *et al.*[21] studied the formation of ternary europium(III) complexes with 4,4,4-trifluoro-1-(2-thienyl)-1,3-butanedione (Htta) and 4,7-diphenyl-1,10-phenanthroline disulfonate formed at

DOI: 10.1039/b507830j

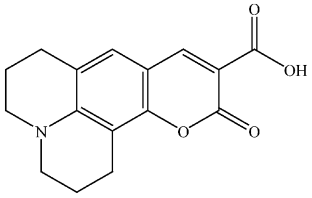

Fig. 1 The structure of C343 dye molecule.

the toluene/water interface using time-resolved TIR fluorescence spectrometry. The double-exponential decay of the fluorescence decay profile of the interfacial complexes was attributed to the existence of two different species. Ishizaka *et al.*[5,22] studied the hybridization of complementary single-stranded DNAs (ssDNA) at a water/CCl_4 interface. Complementary ssDNAs dissolved in water were shown to produce the relevant double-stranded DNA (dsDNA) at a water/CCl_4 interface in the presence of octadecylamine (ODA) in the oil phase. Teramae and coworkers[23] have studied solvent relaxation processes of 12-(9-anthroyloxy)stearic acid (12-AS) and 4-(9-anthroyloxy)butanoic acid (4-ABA) at the heptane/water interface. In a bulk heptane solution, both 12-AS and 4-ABA have shown time-dependent fluorescence spectral shifts, and the decay profiles were analyzed by the two-state kinetics model. Their results indicated a preferential solvation for 12-AS at the heptane/water interface.

In a previous paper we have studied the interfacial properties of C343 dye molecules at the water/DCE interface using surface sensitive second harmonic generation (SHG) and quasi-elastic laser scattering (QELS) techniques.[24] The anomalous pH dependence of SHG signal from C343 at the water/DCE interface was attributed to the intramolecular hydrogen bonding along with the aggregation of the dye molecules at the interface.

In this study, we present preliminary results of time-resolved photophysical properties of C343 (Fig. 1) adsorbed at the water/DCE interface. The eventual aim of these studies is to understand the excited state dynamical properties of the probe molecules at the interfaces. One of the aims of the present study is to compare and contrast the dynamical information obtained for C343 molecules at the water/DCE interface with those obtained in the bulk solution. Our work clearly demonstrates that the dynamical properties at the water/DCE interface differ from that in the bulk solution. The bi-exponential behavior of fluorescence decay of C343 at the interface is attributed to the monomer and aggregate formation. The quenching in monomer fluorescence lifetime at the interface is discussed in terms of excitation energy migration. The paper is organized as follows: in section 2, a detailed description of the apparatus used for the time-resolved measurements is given; in section 3, the steady state and the time domain data are presented and discussed.

2. Experimental

The time-resolved fluorescence decay measurements were performed using the time-correlated single photon counting (TCSPC) technique. The block diagram of the TCSPC set-up developed in our laboratory is shown in Fig. 2. The femtosecond laser pulses of 80 MHz, tunable from 700–1000 nm from the mode locked Ti:sapphire laser (Spectra Physics, Tsunami), pumped by a Nd:YVO_4 solid state laser (Spectra Physics, Millennia Xs), were directed to the pulse picker (Spectra Physics, model 3980). The pulse picker gave frequency doubled output pulses of variable repetition rates. For the present study the repetition rate of the optical pulses was set at 800 kHz. The excitation laser beam was s-polarized using a polarizer and was irradiated onto the water/DCE interface through the DCE phase. The incident angle (θ_i) of the excitation beam was set larger than the critical total reflection angle (θ_c) for the TIR fluorescence spectroscopic measurements at the water/DCE interface ($\theta_c = 67.6^\circ$), whereas for normal excitation, θ_i was set much smaller than θ_c. The deviation in angle caused by the sample is not taken into account for the θ_i values reported in the present study. The fluorescence was collected along the surface normal and its polarization was set at magic angle (54.7°) using another polarizer for the fluorescence decay measurements. The polarized fluorescence was dispersed using a monochromator (Jobin Yvon, H-10) and detected by a microchannel plate photomultiplier (MCP-PM, Hamamatsu, R3809U-50) which was inserted inside the peltier cooled housing. The temperature of the MCP-PM housing was set at −20 °C to minimize the dark counts from the MCP-PM. The output of MCP-PM was further amplified using an amplifier (Becker & Hickl GmbH) and analyzed by a single photon counting module (Edinburgh Instruments, TCC900). The time to amplitude converter (TAC) of TCC900 module was operated in reverse mode, where the signal cable carrying the high count rate from the laser source was connected to the STOP input and the low rate from the MCP-PM was connected to the START input of the TCC900 module. The TCC900 module was operated *via* the dedicated T900 software. The constant fraction discriminator (CFD) parameters *i.e.* threshold, zero crossing level and divider were optimized using T900 software to get the best fit and lifetimes for the fluorescence lifetime standard molecules. The overall instrumental response function, as recorded by scattering the excitation light using water in a sample cell, was around 60 ps full width at half maximum. The laser pulse STOP synchronization was performed by using the laser fundamental beam from the pulse picker and detected using optical trigger OT900 (+15 V bias, rise-time 450 ps). The numerical procedure behind the search for the best lifetime parameters was the Marquardt–Levenberg algorithm, which searches for the best values by the minimization of the 'goodness of fit' χ^2, residuals and the Durbin–Watson (DW) parameters. For the best fit χ^2 must be around 1.0, DW values must be larger than 1.7 for the single exponential fit and 1.75 for the double exponential fit.

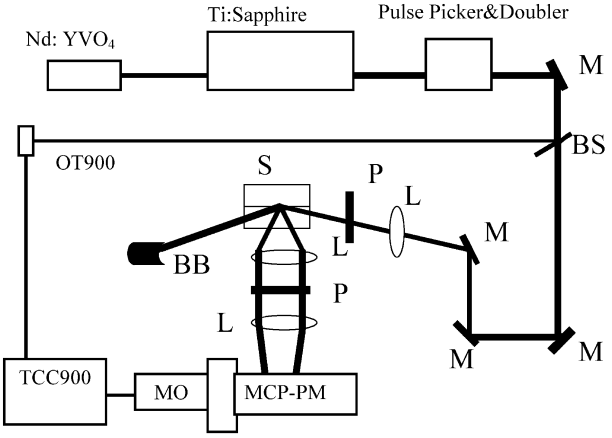

Fig. 2 Schematic of time-correlated single photon counting (TCSPC) set-up for the measurement of fluorescence dynamics under total internal reflection mode at liquid/liquid interface. Key: M mirror, BS beam splitter, L lens, P polarizer, S sample, BB beam blocker, MCP-PM microchannel plate photomultiplier, MO monochromator, OT900 optical trigger module, TCC900 computer module for time-correlated single photon counting.

The bulk steady state absorption spectrum was recorded with a Cary 2400 UV-Vis-NIR spectrophotometer and fluorescence spectra were measured with a home-built spectrofluorometer.[25] The fluorescence spectrum at the water/liquid interface was measured using the TCSPC setup shown in Fig. 2 by measuring the photon count rates at different emission wavelengths.

For TIR experiments the sample was prepared in a 4.0 × 2.0 cm^2 rectangular glass cell. The cell was washed thoroughly with DCE and then with water prior to sample preparation. The C343 dye was dissolved in aqueous phase. All the experiments were carried out using freshly prepared samples. All the reagents employed were of analytical grade. Water was purified by reverse osmosis followed by ion exchange (Millipore, Milli-Q SP reagent system). The 1,2-dichloroethane (Merck, extra pure), and C343 (Aldrich) were used as received.

3. Results and discussion

3.1 Adsorption of C343 at the water/DCE interface

Before doing any photophysical measurements at the water/DCE interface, it was necessary to ascertain that the C343 molecules were adsorbed at the interface. Using the surface sensitive technique of second harmonic generation (SHG) and QELS we have studied the adsorption behavior of C343 at the water/DCE interface and the results have already been reported.[24] Briefly, the SHG intensity was monitored as a function of bulk aqueous concentration of C343. The plot of square root of second harmonic intensity against the concentration of C343 yielded the adsorption isotherm of the molecule. The bulk aqueous concentration was varied from zero to 0.2 mM. The full monolayer coverage was obtained at a bulk aqueous concentration of about 30 μM. The adsorption isotherm exhibited a simple Langmuir isotherm behavior and was an indication of weak interactions among the C343 species adsorbed at the water/DCE interface.

3.2 Steady state measurements

The steady state spectroscopy of C343 depends strongly on its environment.[25–30] Fig. 3 shows the steady-state absorption and fluorescence spectra of C343 in an aqueous bulk solution and at the water/DCE interface. In bulk aqueous solutions the absorption and the emission maxima of C343 are at 428 and 491 nm, respectively, and are in agreement with the reported values.[25,26] However, the peak position of the TIR fluorescence spectrum at the interface is slightly red shifted compared to that of the fluorescence spectrum in the bulk water.

Clearly, the TIR emission spectrum of C343 at the water/DCE interface indicates that the environment sensed by C343 molecules at the interface differs from that in the bulk water solution. The emission spectrum of C343 peaks at slightly longer wavelengths at the water/DCE interface compared to that in bulk water solution. The observed red shift in the emission spectrum can be explained by different possible arguments. First, the red shift observed in surface spectrum may be due to the change in polarity at the interface. Using SHG spectroscopic technique, Wang *et al.*[31] reported that the polarity of the water/DCE interface was equal to the arithmetic average of the adjoining bulk phase. Ishizaka *et al.*[32] investigated the polarity of the water/oil interface by means of time resolved TIR fluorescence spectroscopy of a sulforhodamine B. For the oil having low polarity, the polarity of the water/oil interface agreed with the average of the polarities of the two phases, whereas for the oil having relatively high polarity solvent, the interfacial polarity was less than the average polarities of the two phases. The difference in polarities at the interface was discussed in terms of thickness and roughness of the interface and it was demonstrated that the water/DCE interface is rough and sharp. In a molecular dynamics computer simulations study in which the probe molecule is assumed to be located at the interface of an oil side, Michael and Benjamin [33] reported that the interfacial polarity at a rough interface became higher than that at a sharp interface. Thus the higher polarity of the rough interface of water/DCE could shift the fluorescence spectrum towards the longer wavelengths. Second, the strong interactions among the closely packed dye molecules at the interface could result in red shift in the emission spectrum. However, the adsorption isotherm we have studied for C343 molecules in a previous study[24] followed a simple Langmuir adsorption isotherm which has ruled out the strong interactions among the adsorbed dye molecules at the interface. Third, the red shift in fluorescence spectrum could be due to the protonation of dye at the interface. There are reports[25,26] in the literature about the shift of peak position of the emission spectrum of bulk C343 from 487 nm in neutral or basic solution to 494 nm in acidic solution, and this red shift in emission spectrum has been attributed to the protonation of the dye molecule in the acidic solution. There are several sites on the C343 molecule that could potentially accept a proton: the carboxylic acid group, the cyclic ester and cyclic amine moieties. Riter *et al.*[25] observed that for the lower values of pH, C343 molecules get protonated on the carboxylic acid moiety. Fourth, the red shift can be simply due to the aggregation of dye molecules at the interface.

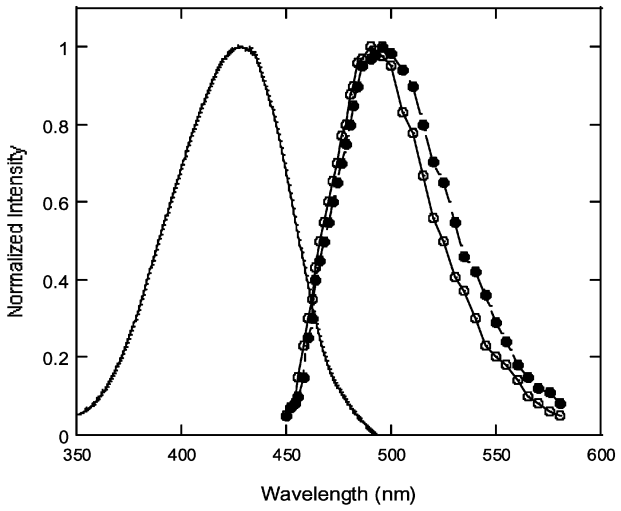

Fig. 3 Steady state absorption (solid line) and emission spectra of C343 (30 μM) in aqueous solution (open circles: bulk water, filled circles: liquid/liquid interface).

Aggregation of C343 dye molecules has been observed for the molecules adsorbed at the surfaces of nanoparticles.[28] The absorption spectra of C343 attached with ZrO_2 nanoparticles showed a dramatic change with the dye concentration. The observed large blue shift in the absorption spectra with the dye concentration has been attributed to the H-aggregation of the dye molecules at the surface. The pH dependence of the SHG signal from C343 at the water/DCE interface showed that for pH 8 and lower, dye was adsorbed at the interface in J-aggregated protonated form. At pH 9 and pH 10, the dye was present in both the protonated and deprotonated form at the interface, whereas at pH 11, the dye molecules were present in the H-aggregated deprotonated form at the interface.[24] The pK_a value at the interface was greater than eight, some four units greater than the pK_a of C343 in bulk aqueous solution, and was attributed to the intramolecular hydrogen bonding along with the aggregation of the dye molecules at the interface. In agreement with our SHG measurements,[24] we conclude that the observed red shift in the emission spectrum in the present study is due to the aggregation of C343 dye molecules at the water/DCE interface. This conclusion is further supported by the TIR fluorescence lifetime measurements at the water/DCE interface and discussed in the following sections.

3.3 Fluorescence lifetime measurements

3.3.1 In bulk water. Fig. 4 shows a fluorescence decay profile of C343 in bulk water under normal conditions. The

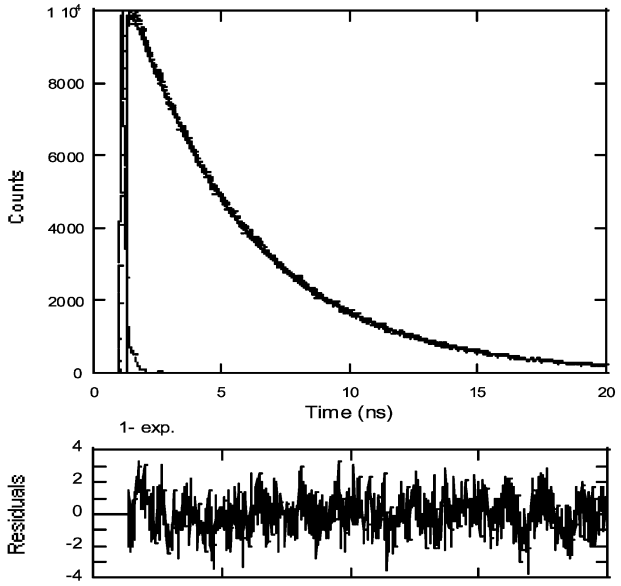

Fig. 4 Fluorescence decay profile of 30 μM C343 in bulk water. The solid curve shows the best fit by eqn (1). The fastest decay profile illustrates an instrument response. The lower panel represents the plot of the weighted residuals for a single exponential fit. Observation wavelength was 460 nm.

fluorescence decay curve fits nicely with a single exponential function:

$$I(t) = \alpha \exp(-t/\tau) \qquad (1)$$

with fluorescence lifetime $\tau = 4.5$ ns and is in agreement with the reported values in the literature. Ghosh[34] carried out fluorescence lifetime measurements for C343 in bulk water. The fluorescence decay analysis for C343 in water gave single exponential fitting with fluorescence lifetime = 4.6 ns and was found to be independent of emission wavelength. Further, it was observed that the emission lifetime of C343 did not change much with the change in solvent. In ethanol, acetonitrile, dichloromethane and acetone, the emission decay traces have been fitted well with single exponential decay function. Using the TCSPC technique, Riter *et al.*[35] observed that the fluorescence lifetime of C343 in the 1 M Na^+ solution was single exponential with the fluorescence lifetime component of 4.5 ns.

3.3.2 At water/DCE interface. Fig. 5 shows a fluorescence decay profile of C343 adsorbed at the water/DCE interface, together with the relevant weighted residuals for the single and double exponential fits. In contrast to the result shown in Fig. 4, the fluorescence decay curve of C343 at the water/DCE interface was fitted well with a double exponential function:

$$I(t) = \alpha_1 \exp(-t/\tau_1) + \alpha_2 \exp(-t/\tau_2) \qquad (2)$$

where τ_1 and τ_2 are the shorter and longer lifetime components, respectively, and α_1 and α_2 are the corresponding amplitudes. The nonrandom distributions of residuals in particular for the single exponential fit in the initial stage of excitation and the randomly distributed residuals for the double exponential fit reveal the bi-exponential nature of the decay curve at the water/DCE interface. The bi-exponential fit is further supported by the χ^2 and the DW parameters. The decrease in χ^2 from 2.1 for the single exponential fit to 1.2 for the double exponential fit is convincing evidence for the non-single exponential decay of C343. The fluorescence decay analysis for C343 at the water/DCE interface under TIR gave τ_1 and τ_2 fluorescence lifetime components 300 and 3600 ps, respectively.

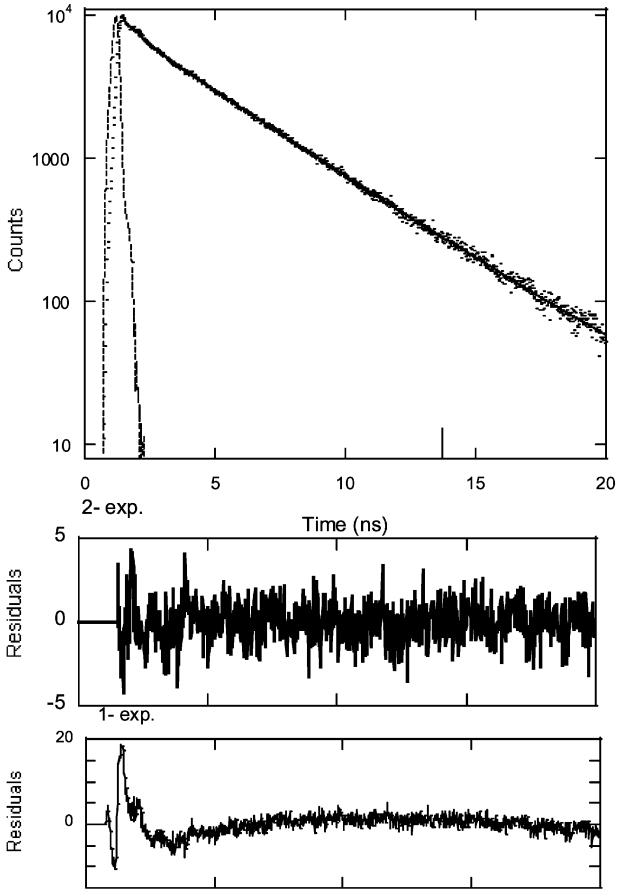

Fig. 5 Fluorescence decay profile of 30 μM C343 at a liquid/liquid interface. The solid curve shows the best fit by eqn (2). The fastest decay profile illustrates an instrument response. The lower panel represents the plot of the weighted residuals for double and single exponential fits. Observation wavelength was 460 nm.

The existence of two fluorescence lifetime components implies that C343 molecules are present in two different forms in the vicinity of the water/DCE interface. The longer fluorescence lifetime component τ_2 (3.6 ns), is closer to the lifetime of C343 species in bulk water and can be assigned to the emission from the monomer molecules of C343. However, a large difference between the shorter lifetime component τ_1 (300 ps) and the fluorescence lifetime in the bulk aqueous solution (4.5 ns) implies that the properties of such C343 species are quite different from those in the bulk aqueous solution. The decrease in fluorescence lifetime is a characteristic of aggregation of dye molecules. In agreement with the conclusion drawn earlier from the steady state measurements, the C343 species having the shorter lifetime component can be ascribed to aggregation of dye molecules at the water/DCE interface. Aggregation is expected to play an important role in fluorescence lifetime quenching of the molecules and has been reported in many publications.[1,4,17,36] The aggregation of merocyanine dye at the solid/liquid interface layer was enhanced in the interface layer of up to 100 nm thickness compared to that in the bulk solution.[1] The aggregation state of pyrene molecules between interface and bulk layers was compared and it was observed[36] that the excimer fluorescence decayed faster under the TIR condition compared to the normal condition. The excited state monomer and the excimer near the interface were quenched more efficiently by the non-fluorescent dimers compared to those in the bulk solution. Avis and Porter[37] proposed the presence of non-fluorescent dimers leading to quenching of both the monomer and excimer fluorescence of pyrene doped PMMA films.

3.4 Aqueous phase penetration depth dependence of decay parameters

The depth of penetration (d_p) depends on the incident wavelength (λ_i), the angle of incidence (θ_i), and the refractive index ratio, n_2/n_1[4,17,36]:

$$d_p = \frac{\lambda_i}{4\pi n_1 \sqrt{\left(\sin^2\theta_i - \frac{n_2^2}{n_1^2}\right)}} \quad (3)$$

The evanescent wave is a stationary electromagnetic wave initiated at the interface and the intensity of this stationary wave in the aqueous phase decays exponentially with distance from the interface. Thus the fluorescence intensity $I(z)$ at any depth z from the interface is given by[36]

$$I(z) = CI_0 \exp(-z/d_p) \quad (4)$$

In this expression I_0 is the light-intensity of the evanescent wave at the interface and C is a constant which depends on the fluorophore, its quantum yield, and the experimental conditions used. As a result, the properties of the interface region around the probe molecule at the interface layer can be investigated through the fluorescence behavior of the probe molecule. A series of fluorescence decay curves were recorded at different incident angles in order to evaluate the location of the dye aggregates in the interfacial region. The fluorescence intensity of C343 decreased sharply upon a slight increase of incident angle. The relative fluorescence intensity was very sensitive to the incident angle, and changed by 1 order of magnitude, corresponding to an increase of incident angle by about 1°. TIR occurs when θ_i exceeds θ_c, which is given by:

$$\theta_c = \sin^{-1}\left(\frac{n_2}{n_1}\right) \quad (5)$$

In the present study, the organic phase is DCE with $n_1 = 1.4421$ and the aqueous phase is water with $n_2 = 1.3330$, resulting in $\theta_c = 67.6°$. Fig. 6 shows the fluorescence decay profiles of C343 at the water/DCE interface for different incident angles of excitation. Clearly, the decay profiles change successively with the change in angle of incidence. For the normal excitation condition, the recorded decay curve is the same as the decay curve shown in Fig. 4 for the bulk aqueous solution and fits nicely with single exponential function, whereas the decay curves obtained under TIR condition are non-exponential and analyzed with double exponential function using eqn (2). In order to determine the relative fluorescence intensity contribution of the individual lifetime components to the total fluorescence intensity, we calculated the normalized relative amplitudes A_1 and A_2 from the observed fluorescence decay times and pre-exponential factors using the following equations:

$$A_1 = \left(\frac{\alpha_1\tau_1}{\alpha_1\tau_1 + \alpha_2\tau_2}\right),$$
$$A_2 = \left(\frac{\alpha_2\tau_2}{\alpha_1\tau_1 + \alpha_2\tau_2}\right) \quad (6)$$

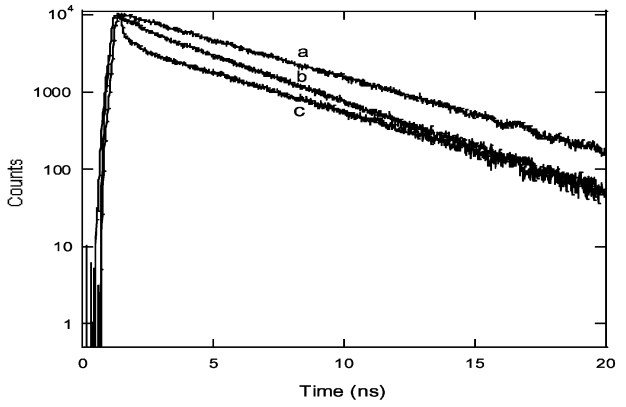

Fig. 6 Fluorescence decay profiles of 30 μM C343 at the water/DCE interface as a function of penetration depth observed at 460 nm: (a) normal conditions ($\theta_i = 50°$), (b) TIR condition ($\theta_i = 70°$), (c) TIR condition ($\theta_i = 73°$).

Table 1 Fluorescence decay parameters of C343 as a function of penetration depth of the aqueous phase

Angle of incidence θ_i	Penetration depth/nm	τ_1/ps	τ_2/ps	A_1	A_2	χ^2
70	138	330	3620	4	96	1.2
71.5	110	300	3600	5	95	1.3
72	104	350	3630	6	94	1.4
72.5	99	310	3700	14	86	1.5
73	95	350	3650	27	73	1.3

All the data related to penetration depth are summarized in Table 1. Interestingly, the observed fluorescence lifetime decay components are little affected by the incident angle, whereas the normalized amplitudes change significantly with the change in incident angle. The amplitude corresponding to shorter lifetime component increases and the amplitude corresponding to longer lifetime component decreases with the decrease in penetration depth of the aqueous phase from the interface. As it has been reported[38] that the thickness of a sharp liquid/liquid interface represented by a 1,2-dichloroethane interface is around 1 nm, the penetration depth (dp) of the incident evanescent wave, even for the largest θ_i studied in the present study is thicker than the interfacial layer of water/DCE. Consequently, under TIR condition, the observed fluorescence decay curves have contribution both from C343 molecules in aqueous bulk phase and C343 molecules adsorbed at the water/DCE interface. Thus for any angle of incidence under TIR condition, we probe both monomer and the aggregate species of C343. However, the concentration of monomer species probed decreases and that of the aggregates increases with the decrease in penetration depth of the aqueous phase from the interface.

The amplitude ratio of aggregates to the monomer, A_1/A_2, is plotted as a function of penetration depth in Fig. 7. With a decrease in penetration depth of the aqueous phase from the interface, the ratio of aggregate to monomer is increased, indicating that the aggregation is significantly prominent nearer to the interface layer. The observed relatively enhanced aggregation of C343 dye molecules near the interface could be due to the favorable orientation of adsorbed dye molecules to

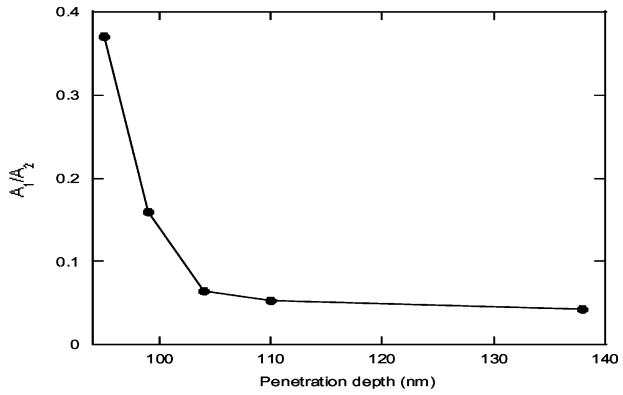

Fig. 7 The penetration depth dependence of A_1/A_2 for C343 (30 μM) at the water/DCE interface.

make the aggregation process more efficient in the interfacial layer.

According to the simple theory of aggregate decay dynamics,[39] if the radiative decay rate of an isolated two-level single molecule is γ, and the size of aggregate includes N such molecules, the radiative decay rate of the aggregate is determined by $N\gamma$. Thus the lifetime of an aggregate is N times smaller than that of a single molecule. From the ratio of the lifetime of the aggregate to the monomer, we estimated that 10 molecules of C343 participated in the formation of an aggregate at the interface. This result demonstrates that the size of aggregation of C343 at the water/DCE interface is quite large.

It should also be noted that the fluorescence lifetime of monomers is shorter at the interface compared to that in the bulk solution. One possible way to explain the origin of the quenching in monomer fluorescence lifetime at the interface might be to assume excitation energy migration between the C343 molecules at the water/DCE interface. The efficiency of energy migration strongly depends on the orientation and the spacing between the molecules. As for the present system, the adsorbed C343 molecules at the water/DCE interface have net orientation and are closely spaced,[24] thus we can assume that the distance between the molecules adsorbed at the interface was under the critical energy transfer distance and the orientation of adsorbed C343 molecules made the favorable geometry for the energy transfer. In solutions, the excited state of the molecular ensemble can be considered as a distribution of quasi-continuum excited states. The emission from a higher state can overlap with the absorption transition to a lower lying state, making conditions for excitation energy transfer favorable, particularly for the monomer molecules closely spaced and adsorbed at the interface. The degradation of energy in this manner ultimately terminates into the emission from the lowest level of the system. Such an energy transfer, known as energy migration, results in a decrease in the fluorescence lifetime. Scully *et al.*[40] found that the fluorescence lifetime quenching of Rhodamine 6G dimers was enhanced by excitation energy migration between monomers. Chen and Knutson[41] studied carboxyfluorescein using time-resolved spectroscopy and it has been observed that the fluorescence lifetimes decreased with increase in dye concentration. The observation was explained as a consequence of dimerization and excitation energy transfer to dimmer facilitated by energy migration between monomers. The fluorescence decays of disulfonated aluminium phthalocyanine have been analyzed[42] using a model which assumes excitation energy migration between diffusing monomers and quenching by diffusing dimers. The occurrence and the nature of fluorescence decay dynamics of C343 at the water/DCE interface as observed above are in conformity with the energy migration process among the C343 monomers at the water/DCE interface.

4. Conclusions

We have studied the fluorescence decay kinetics of C343 at the water/DCE interface using TIR time-resolved fluorescence spectroscopy. In contrast to fluorescence decay of C343 in bulk aqueous solution, the decay at the interface is non-exponential with two fluorescence lifetimes. The shorter lifetime component is attributed to the aggregation of the dye molecules at the interface, whereas the longer lifetime component is from the monomers of C343. On decreasing the penetration distance of aqueous phase from the interface, the decay curves become increasingly more non-exponential with constant average lifetime. The amplitude corresponding to the shorter lifetime component increases, whereas the amplitude corresponding to longer lifetime component decreases with the decrease in penetration distance and clearly demonstrates the promotion of aggregation process around the interface layer. The monomer fluorescence lifetime of C343 at the interface was found quenched compared to that in the bulk aqueous solution and interpreted in terms of excitation energy migration among the monomers at the interface. Further systematic investigations of dye concentration dependence of fluorescence decay kinetics and dynamic fluorescence anisotropy measurements at the interface are being undertaken to clarify the more exact picture of aggregation behavior of C343 molecules at the interface and will provide direct evidence for the excitation energy migration between the monomers. Also, the results obtained in the present study are limited to the water/DCE interface; analogous studies will be extended to other systems to reveal the effect of interfacial structure on the fluorescence dynamics.

Acknowledgements

We gratefully acknowledge funding from EPFL and the Fonds National de la Researche Scientifique.

References

1 S. Hamai, N. Tamai and H. Masuhara, *Chem. Lett*., 1993, **1105**.
2 S. Hamai, N. Tamai, M. Yanagimachi and H. Masuhara, *Chem. Phys. Lett*., 1994, **229**, 389.
3 S. Harlepp, J. Robert, N. C. Darnton and D. Chatenay, *Appl. Phys. Lett*., 2004, **85**, 3917.
4 S. Hamai, N. Tamai and H. Masuhara, *J. Phys. Chem*., 1995, **99**, 4980.
5 S. Ishizaka, Y. Ueda and N. Kitamura, *Anal. Chem*., 2004, **76**, 5075.
6 S. Ishizaka and N. Kitamura, *Anal. Sci*., 2004, **20**, 1587.
7 H. Masuhara, N. Mataga, S. Tazuke, T. Murao and I. Yamazaki, *Chem. Phys. Lett*., 1983, **100**, 415.
8 H. Masuhara, S. Tazuke, N. Tamai and I. Yamazaki, *J. Phys. Chem*., 1986, **90**, 5830.
9 S. Phimphivong, S. Koelchens, P. L. Edmiston and S. S. Saavedra, *Anal. Chim. Acta*, 1995, **307**, 403.
10 H. Schneckenburger, *Curr. Opin. Biotechnol*., 2005, **16**, 13.
11 Y. Taniguchi, M. Mitsuya, N. Tamai, I. Yamazaki and H. Masuhara, *J. Colloid Interface Sci*., 1985, **104**, 596.
12 N. L. Thompson and J. K. Pero, *Springer Ser. Fluoresc*., 2005, **3**, 79.
13 M. Toriumi and H. Masuhara, *Spectrochim. Acta Rev*., 1991, **14**, 353.
14 M. Yanagimachi, N. Tamai and H. Masuhara, *Chem. Phys. Lett*., 1993, **201**, 115.
15 H. Yao, F. Kitagawa and N. Kitamura, *Langmuir*, 2000, **16**, 3454.
16 M. Yanagimachi, N. Tamai and H. Masuhara, *Chem. Phys. Lett*., 1992, **200**, 469.
17 S. Hamai, N. Tamai and H. Masuhara, *Chem. Phys. Lett*., 1993, **213**, 407.
18 S. Hamai, N. Tamai and M. Yanagimachi, *Microchem. Proc. JRDC-KUL Jt. Int. Symp*., 1994, 335.
19 S. Phimphivong and S. S. Saavedra, *Bioconjugate Chem*., 1998, **9**, 350.
20 K. Bessho, T. Uchida, A. Yamauchi, T. Shioya and N. Teramae, *Chem. Phys. Lett*., 1997, **264**, 381.
21 M. Fujiwara, S. Tsukahara and H. Watarai, *Phys. Chem. Chem. Phys*., 1999, **1**, 2949.
22 S. Ishizaka, Y. Ueda and N. Kitamura, *Anal. Chem*., 2004, **76**, 5075.
23 T. Yamashita, T. Uchida, T. Fukushima and N. Teramae, *J. Phys. Chem. B*, 2003, **107**, 4786.
24 D. Pant, M. Guennec, B. Illien and H. H. Girault, *Phys. Chem. Chem. Phys*., 2004, **6**, 3140.
25 R. E. Riter, E. P. Undiks and N. E. Levinger, *J. Am. Chem. Soc*., 1998, **120**, 6062.
26 K. Tominaga and G. C. Walker, *J. Photochem. Photobiol., A: Chem*., 1995, **87**, 127.
27 D. Pant and N. E. Levinger, *Langmuir*, 2000, **16**, 10123.
28 D. Pant and N. E. Levinger, *J. Phys. Chem. B*, 1999, **103**, 7846.
29 D. Pant, R. E. Riter and N. E. Levinger, *J. Chem. Phys*., 1998, **109**, 9995.
30 D. Pant and N. E. Levinger, *Chem. Phys. Lett*., 1998, **292**, 200.
31 H. Wang, E. Borguet and K. B. Eisenthal, *J. Phys. Chem. B*, 1998, **102**, 4927.
32 S. Ishizaka, H.-B. KIm and N. Kitamura, *Anal. Chim*., 2001, **73**, 2421.
33 D. Michael and I. Benjamin, *J. Phys. Chem*., 1998, **102**, 5145.

34 H. N. Ghosh, *J. Phys. Chem*., 1999, **103**, 10382.
35 R. E. Riter, D. M. Willard and N. E. Levinger, *J. Phys. Chem*., 1998, **102**, 2705.
36 A. Itaya, Y. Matsumoto, I. Iou, H. Masuhara and F. C. De Schryver, *Polymer*, 1994, **35**, 3920.
37 P. Avis and G. Porter, *J. Chem. Soc., Faraday Trans*., 1974, **70**, 1057.
38 I. Benjamin, *J. Chem. Phys*., 1992, **97**, 1432.
39 J. Grad, G. Hernandez and S. Mukamel, *Phys. Rev. A*, 1988, **37**, 3835.
40 A. D. Scully, A. Matsumoto and S. Hirayama, *Chem. Phys*., 1991, **157**, 253.
41 R. F. Chen and J. R. Knutson, *Anal. Biochem*., 1988, **172**, 61.
42 Z. Petrasek and D. Phillips, *Photochem. Photobiol. Sci*., 2003, **2**, 236.